

## **No long-range magnetic order in $\epsilon$ -Iron down to 160 mK**

S. Klotz<sup>1\*</sup>, M. d'Astuto<sup>2</sup>, V. Joyet<sup>3</sup>, H. Kobayashi<sup>1,4</sup>, E. Lelièvre-Berna<sup>3</sup>, J. Maurice<sup>3</sup>, C. Payre<sup>3</sup> S. Savvin<sup>3,5</sup>

- 1) IMPMC, Sorbonne Université, CNRS 7590, 4 Place Jussieu, 75252 Paris, France
- 2) Institut Néel, 25 Avenue des Martyrs, 38042 Grenoble, France
- 3) Institut Laue-Langevin, 71 Avenue des Martyrs, 38042 Grenoble, France
- 4) The University of Tokyo, 7-3-1 Hongo, Bunkyo-ku, Tokyo 113-0033, Japan
- 5) Instituto de Nanociencia y Materiales de Aragón, CSIC – Universidad de Zaragoza, Facultad de Ciencias C/ Pedro Cerbuna 12, Zaragoza, Spain

### **Abstract**

Epsilon-Fe, the high-pressure phase of elemental iron, is generally regarded as non-magnetic. However, theoretical predictions and experiments suggest that a residual magnetic moment exists, which might order at sufficiently low temperatures. Here we report neutron diffraction data at 20 GPa down to 160 mK to probe this possibility. We find no magnetic long-range order under these conditions and no evidence for magnetic diffuse scattering, a result which considerably constrains the size of the magnetic moment, the nature of the putative magnetic order and its stability range.

Keywords: iron, high pressure, magnetism, low temperatures

\*) e-mail: Stefan.Klotz@upmc.fr

Iron is one of the most abundant and stable elements in the universe. Under compression, it transforms at 14-20 GPa from the body centered cubic (bcc)  $\alpha$ -phase to the hexagonal close-packed (hcp)  $\epsilon$ -form [1]. This transition has been extensively studied in the past, mainly because  $\epsilon$ -iron is the major component of the Earth's core. Epsilon-iron is generally believed to be "non-magnetic", i.e. either paramagnetic or completely nonmagnetic with zero spin. This is essentially based on early Mössbauer studies at 19 GPa and down to 30 mK which did not detect a hyperfine splitting which could testify of a local magnetic field [2,3]. However, theory and various indirect experimental findings suggest the existence of a remanent magnetic moment in  $\epsilon$ -Fe and hence the possibility of magnetic ordering at low temperatures [4-10]. Raman data find an unexpected splitting of the TO mode at 20-30 GPa [4,5] and  $K\beta$ -X-ray emission spectra (XES) and x-ray circular dichroism data [6,7] can be interpreted as arising from a magnetic moment. Also, resistivity measurements show an unusual power law in the temperature dependence which indicates para- or ferromagnetism [8], and this seems to be supported by susceptibility measurements at 300 K [9]. First-principles calculations [10] have indeed proposed an antiferromagnetic ground state which is able to explain both the Mössbauer and the Raman results. This model was recently refined by including longitudinal spin modulations which leads to a so-called "spin-smectic" ground state [6]. In all cases theory suggests a sizable moment of 0.5-1  $\mu_B$ . To resume, the magnetic state of  $\epsilon$ -iron is controversial related to the difficulty to carry out direct and unambiguous experiments at such extreme pressure-temperature conditions.

In this work we present neutron diffraction data of  $\epsilon$ -iron at 20 GPa at very low temperatures down to 160 mK. It extends our previous findings obtained at temperatures down to 1.8 K [6] by more than one order of magnitude and reduces thereby considerably the possibility of magnetic order in  $\epsilon$ -Fe. Neutron diffraction is the most direct and incontestable probe for magnetic long-range order.

The experimental setup consists of a combination of a VX5 Paris-Edinburgh high-pressure device [11] with a dilution cryostat. We used double-toroidal sintered diamond anvils which were made from SUMIDIA WD960 dies from Sumitomo and spark eroded to have a profile as previously published [12]. The sample consisted of a spherical pellet of pure iron (99.995% from Aldrich) and mass of 60 mg (volume: ca. 7.6 mm<sup>3</sup>) which was machined from a rod of 4 mm diameter. No pressure transmitting fluid was used since commonly available fluids are solid anyway at the pressure range of interest (10-20 GPa). We used gaskets made of copper beryllium alloy (NGK BERYLCO 25) because the metal usually employed in high-pressure neutron scattering, null-scattering TiZr, suffers strong embrittlement at low temperatures and pressures beyond 10-14 GPa where a phase transition occurs in this material [13]. This leads to frequent and violent blow-outs, i.e. failures of the gasket resulting in a rapid decompression with a loss of the sample and often also the anvils. Such a risk had to be excluded in a complex and time-consuming experiment as ours. Copper beryllium appeared to be the only safe choice combining high strength, absence of embrittlement and absence of magnetism down to 0 K. Unfortunately, this alloy produces Bragg reflections (i.e. it is not null-scattering) which partly overlap with the strongest nuclear reflections of  $\alpha$ - and

$\epsilon$ -iron. However, the low-Q (low  $2\theta$ ) range where magnetic reflections are expected is completely clear of reflections from gasket and anvils material, as shown further below.

The dilution cryostat hosting the VX5 press is a cryogen-free Triton DR-200 distributed by Oxford Instruments (Fig. 1). The cell is attached to the stage of the mixing chamber and placed inside a tight calorimeter filled with 10-30 mbar of helium gas for increasing the thermalisation. The piston of the press is driven by up to 2 kbar helium gas as in the 3 K PE-cryostat [14]. To reduce the heat load brought to the press, the high-pressure capillary is thermally anchored to all stages of the cryostat with copper braids. At 80 mK, the heat flux into the pressure cell was determined in off-line measurements to be 130  $\mu$ W. The temperature of the sample was measured with Cernox and RuO<sub>2</sub> sensors attached to the top and bottom of the press. The base temperature depends on the settings of the dilution process, the nature of the sample as well as the beam characteristics (neutron flux) of the instrument. There is significant increase in temperature of typically 50-100 mK when the beam shutter is open compared to no beam on the sample. We measured 70 mK during the commissioning phase (off-line) and 130 mK during first test measurements under load. In the current work, temperatures between 150 and 160 mK were reached during measurements and maintained continuously over 3 days. For the sake of simplicity, we quote as base temperature 160 mK throughout this text.

All neutron diffraction measurements were carried out at the recently commissioned XtremeD beamline of the Institut Laue-Langevin (ILL) at Grenoble, France, using a wave length of 2.4446 Å. A detailed description of the instrument can be found elsewhere [15]. The exact value of the wave length is critical for the pressure determination and was obtained from a calibration run using the Na<sub>2</sub>Ca<sub>3</sub>Al<sub>2</sub>F<sub>14</sub> standard. All refinements (including the wave length calibration) were carried out using the FullProf suite (<https://www.ill.eu/sites/fullprof/>).

Pressure was applied at room temperature by injecting up to 1350 bar He into the ram of the Paris-Edinburgh press to generate a force of 90 tons onto the anvils. During the cool-down, this force was maintained by an automatic gas compressor unit, including across the solidification of He in the ram at 17 K.

Figure 2 shows diffraction patterns collected during compression at 300 K, from the ambient pressure bcc phase ( $\alpha$ -Fe) to the high-pressure hcp solid ( $\epsilon$ -Fe). As mentioned further above, the strongest reflections are from the sample environment, i.e. diamond and Cu:Be alloy from the anvils and the gasket, respectively. (The Cu:Be alloy was over-annealed to reach a similar strength as TiZr which leads to the formation of a phase mixture of stoichiometric CuBe with NaCl structure in an almost pure fcc Cu matrix with an additional reflection at  $2\theta=79^\circ$ ). Nevertheless, the  $\alpha$ - $\epsilon$ -phase transition can clearly be observed by the decrease of the strong 110 and 200 bcc Bragg peaks at  $75^\circ$  and  $120^\circ$  and the successive appearance of the 101 and 102 hcp reflections of the  $\epsilon$ -phase at  $80^\circ$  and  $116^\circ$ . At a load of 90 tonnes on the anvils the patterns indicate pure  $\epsilon$ -Fe. A fit to the 101 and 102 reflections gives  $2\theta$  positions of  $81.56 \pm 0.04^\circ$  and  $115.78 \pm 0.08^\circ$  at 300 K as well as  $81.80 \pm 0.05^\circ$  and  $116.38 \pm 0.07^\circ$  at 5 K. From the values we deduce lattice parameters of  $a=2.458(2)$  Å and  $c=3.926(5)$  Å ( $V=10.27(3)$  Å<sup>3</sup>/atom) at 300 K as well as  $a=2.454(2)$  Å and  $c=3.908(5)$  Å ( $V=10.19(3)$  Å<sup>3</sup>/atom) at 5 K. Using the Vinet-equation of state [18] for  $\epsilon$ -Fe established by Dewaele et al. at 300 K [17] ( $V_0=11.214$

$\text{\AA}^3$ ,  $B_0=163.4$  GPa,  $B'=5.38$ ) and 15 K [19] ( $V_0=11.207$   $\text{\AA}^3$ ,  $B_0=163.6$  GPa,  $B'=5.33$ ) results in a pressure of 18.1 GPa at 300 K and 20.0 GPa below 5 K. These values agree well with the previously established load-pressure curve for such anvils [12]. The increase in pressure is likely to have occurred within the first few hours after starting the slow (3 days) cooling process, i.e. above 250 K, probably due to a relaxation in the gasket.

Figure 3(a) shows patterns at base temperature (160 mK) and 5 K, accumulated for 36 and 40 hours, respectively. The 5 K pattern was chosen as a reference as we know from previous data that there is no magnetic long-range order at this temperature [6]. Any magnetic signal, if it exists, should show up below 1.8 K and be visible in the difference curve shown in the lower panel (b). The error bars in the (b) arise from the  $1/\sqrt{N}$  statistics where  $N$  is the number of neutrons in a given channel. Given the fact that theory suggests antiferromagnetic ordering [10, 6], potential magnetic Bragg reflections are expected in the low- $2\theta$  range left to the first nuclear reflections, i.e. below  $80^\circ$ . Figure 3b gives no evidence for this within a precision better than 1%. In fact, the standard deviation of the data from zero is 0.4%, taken over the whole  $2\theta$  range. There is no evidence for ferromagnetic order either, as no change in intensity of the 101 ( $81^\circ$ ) and 102 ( $116^\circ$ ) reflections can be detected.

There is obviously the possibility that long-range magnetic order is not observed because the moments are considerably smaller than predicted by theory. To explore this potential case, we simulated the AFMII structure assuming moments of different magnitude and compare it with the statistical noise in the region of interest, as shown in Fig. 4. Specifically, we take the nuclear (crystal) structure from the Rietveld refinement [20] to the 160 mK data as shown in the inset of Fig. 4, fix its parameters and add the magnetic structure assuming a moment of 0.5, 0.3 and 0.2 Bohr magnetons ( $\mu_B$ ). The main panel of Fig. 4 then shows the difference plots of these three simulations with respect to the simulation with  $m = 0 \mu_B$  (no magnetism), and compares it to the experimental data, i.e. the difference between 160 mK and 5 K patterns. From this we conclude that the detection limit in our measurements is between 0.1 and 0.2  $\mu_B$ . Any ordered magnetic moment below this value would have remained undetected. Note that the intensity of magnetic Bragg reflections varies with the square of the magnetic moment. In fact, magnetic order with moments below typically 0.1  $\mu_B$  are very difficult to detect by non-polarized neutron scattering, even with macroscopic samples at ambient pressure.

A second possibility is that short-range magnetic correlations occur, and no long-range static order, giving rise only to diffuse magnetic scattering without any Bragg reflections. Short-range magnetic correlations are observed frequently above magnetic ordering, or down to 0 K as a result of magnetic frustration. Fluctuations have been suggested for the “spin-smectic” ground state [6].

In the case of short-range magnetic correlations, a simple estimate using Scherrer’s formula shows that the correlation length of a magnetic feature (more exactly the size of the ordered domains) must be larger than 20-30  $\text{\AA}$  to produce a measurable peak broadening at a wave length of 2.445  $\text{\AA}$ . In other words, if the correlations extend over a distance of only several lattice parameters, diffuse magnetic scattering would have remained undetectable in this experiment, even for large moments.

There could be the possibility of fluctuations which may wipe out long-range ordering even in the case of relatively large moments and correlation lengths. Neutron diffraction is sensitive to it if they are slower than the neutron coherence time  $\tau \approx \hbar/2E$  where  $\hbar$  is Heisenberg's constant and  $E$  the energy of the neutron [21]. The neutron coherence time is the time-resolution of a neutron measurement related to the Heisenberg's uncertainty relation in the time-energy domain. In our case this gives  $\tau \approx 2 \times 10^{-14}$  sec which is consistent with the absence of a Mössbauer signal which would be visible for fluctuations slower than  $10^{-7}$  sec [22]. The fact that we do not see any diffuse or Bragg scattering freezing out from such hypothetical fluctuations at 160 mK would hence place a lower limit on their speed on the order of 10-100 fsec. Unfortunately, the "spin-smectic" model [6] gives no time scales in such a scenario which can be compared to experiments. The main reason for the absence of magnetic long-range order is explained by weak inter-layer interactions which then may result in local spin fluctuations.

To summarize, we have presented neutron diffraction data of  $\epsilon$ -iron to unprecedented low temperatures, i.e., 160 mK, which is more than one order of magnitude lower in temperature compared to previous neutron measurements. This has been made possible due to recent developments in cryogenic and high-pressure techniques. We find no evidence of long-range magnetic ordering, ferro or anti-ferromagnetic, contrary to several predictions from first-principles calculations [10, 6]. This result does not necessarily exclude the existence of a remanent magnetic moment in  $\epsilon$ -iron, but considerably reduces various possible scenarios: If there is long range order at 160 mK, the ordered moment has to be smaller than  $\sim 0.2 \mu_B$ , i.e.  $\sim 10$  times lower than in bcc iron and 3-5 times smaller than suggested by theory [10, 6] and XES measurements [6]. If, on the contrary, the moment is larger than this value, magnetic order must be of short-range nature with correlation lengths less than 10-20 Å, i.e. typically a few unit cell distances, or imply also very fast fluctuations, as for example in the case of a "spin-smectic" ground state [6]. To distinguish experimentally between these cases needs a probe which is sensitive to local magnetic fields at positions other than those of the iron nucleus where the hyperfine-field seems to be very small. Muon spin spectroscopy which probes the field at interstitial positions would be an interesting option, though the maximum pressures reachable up to date are limited to approximately 3 GPa [23].

The techniques developed in this work opens promising experimental possibilities for the study of structures and excitations in condensed matter at extreme P/T conditions. Examples include the behavior of magnetically frustrated systems which order close to 0 K [24], the interplay between magnetism and superconductivity [25], and investigations of quantum critical points and other emergent quantum phenomena in condensed matter.

This work was supported by the Young Researchers Overseas Challenge Program (Japan Society for the Promotion of Science), Ludo Frevel Crystallography Scholarship Award 2025 (International Centre for Diffraction Data), and the MERIT-WINGS programme (The University of Tokyo) for H.K.

## AUTHOR DECLARATIONS

### Conflict of interests

The authors declare no conflict of interests

## DATA AVAILABILITY

The data that support the findings of this study are available from the corresponding author upon reasonable request. Neutron diffraction data of this work are available at the Institute Laue-Langevin DataCite <http://dx.doi.org/10.5291/ILL-DATA.5-31-3046>.

### Author contributions

**Stefan Klotz:** Conceptualization (lead), Formal analysis (lead); Funding acquisition (equal); Investigation (equal); Methodology (lead); Project administration (lead); Supervision (lead); Writing (lead). **Matteo d'Astuto:** Conceptualization (equal); Investigation (equal); Writing (equal). **Victorien Joyet:** Investigation (equal); Methodology (equal); **H. Kobayashi:** Investigation (equal); Formal analysis (equal); Writing (equal) **Eddy Lelièvre-Berna:** Investigation (equal), Methodology (equal); Resources (lead); Writing (equal); **James Maurice:** Investigation (supporting), Resources (supporting). **Claude Payre:** Investigation (supporting), Resources (supporting). **Stanislav Savvin:** Investigation (equal); Resources (equal); Writing (equal).

## FIGURES

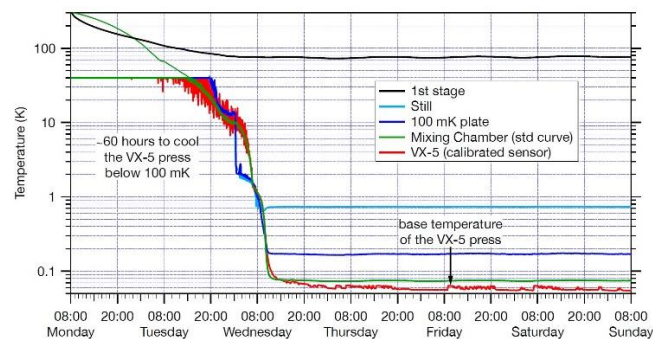
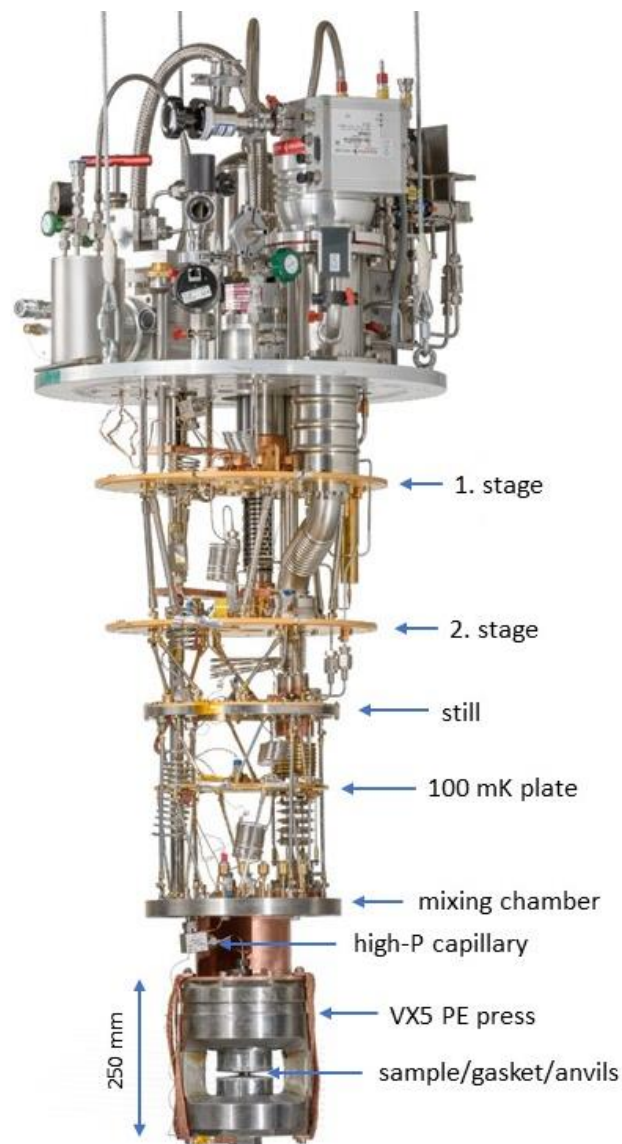


Figure 1. Upper: Internal view of the dilution cryostat hosting a VX5 PE press. The press is suspended to the stage of the mixing chamber with a support made from OFHC copper. To speed up the cool-down and reduce temperature gradients, the press is installed in a tight chamber filled with 20-30 mbar He and its top and bottom faces are thermally linked with Cu braids. Lower: Temperature variations during cooling, measured at different locations during a test run down to 70 mK for several days. Photo ©Ecliptique: L. Thion

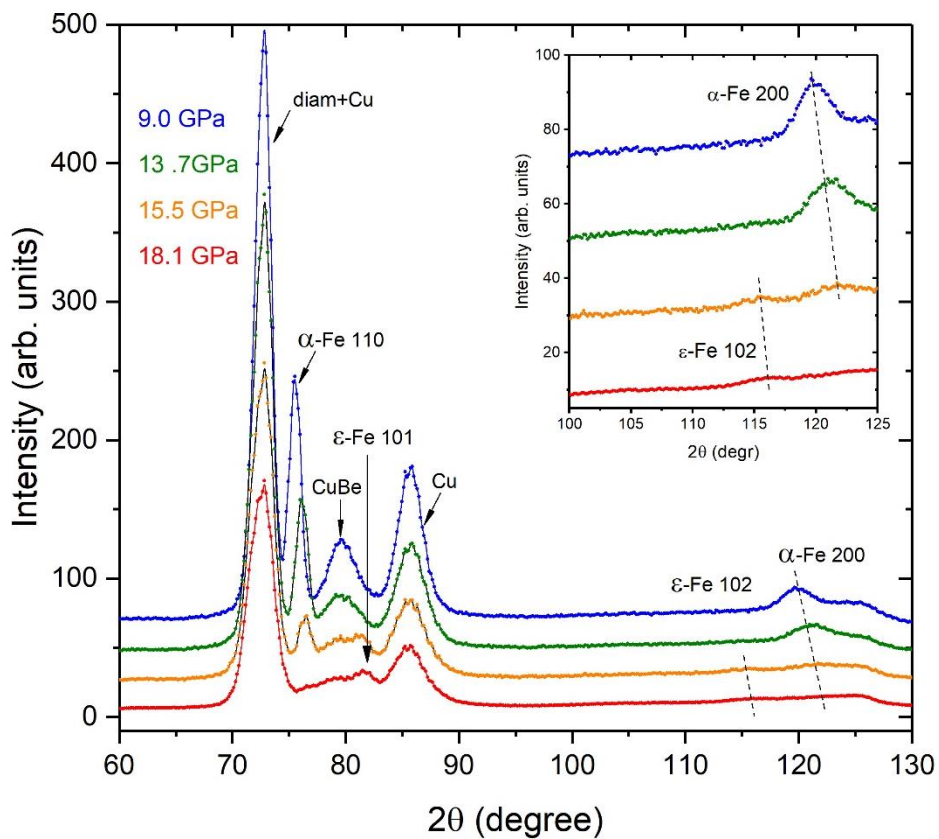


Figure 2: Neutron diffraction patterns of iron upon compression from the ambient-pressure  $\alpha$ -phase to high-pressure  $\varepsilon$ -iron, at 300 K. Curves are shifted by +20 vertically to avoid overlap. Most of the strong reflections are from diamond (anvils) and the gasket material (copper beryllium). Pressure values were determined from the 300 K equations of state of  $\alpha$ -Fe [16] and  $\varepsilon$ -Fe [17].

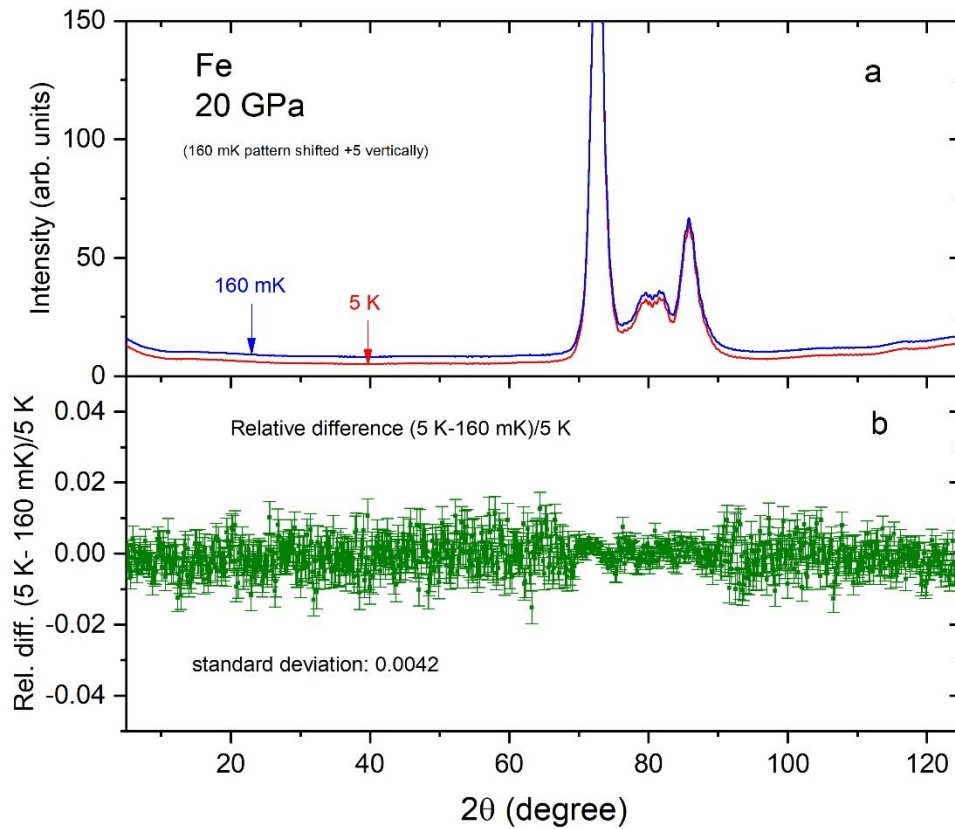


Figure 3: Diffraction patterns of  $\epsilon$ -Fe over the full  $2\theta$  range (panel a), at 5 K (red) and 160 mK (blue). The accumulation time is 36 and 40 h, respectively. The 160 mK patterns were shifted by +5 vertically to avoid overlap. Panel b: Relative difference between 160 mK and 5 K data. The standard deviation over the entire range (863 points) is 0.42%.

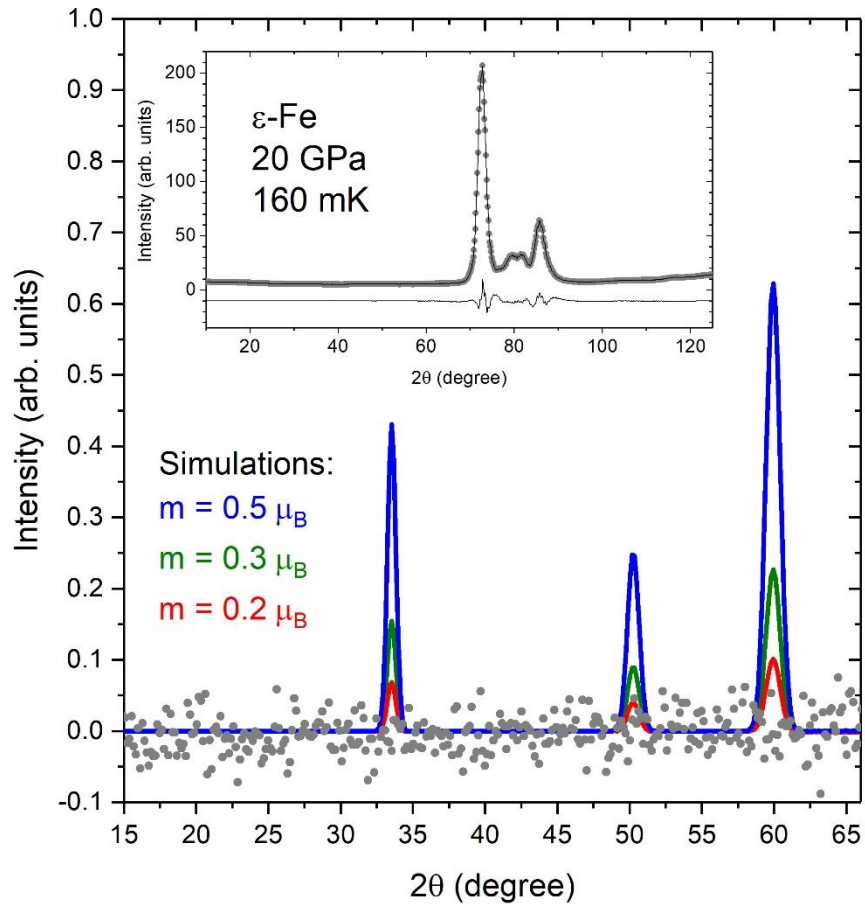


Fig. 4: Main figure: Simulation of magnetic Bragg reflections according to the AFMII structure proposed by theory [10] assuming a magnitude of the magnetic moment  $m$  of 0.5, 0.3 and 0.2 Bohr  $\mu_B$ . The corresponding measured data (5 K – 160 mK patterns) are shown as dots. Inset: Neutron diffraction data (dots) and Rietveld refinement (line through the data) with the difference curve plotted below. The refinements include four phases:  $\epsilon$ -Fe, Cu, Cu:Be alloy and diamond. See fig. 2 for peak assignments.

## REFERENCES

- [1] D. A. Young, *Phase Diagrams of the Elements*, Univ. of California Press, 1991.
- [2] G. Cort, R. Taylor, J. Willis, "Search for magnetism in hcp epsilon-Fe", *J. Appl. Phys.* **53**, 2064–2065 (1982).
- [3], R.D. Taylor, M.P. Pasternak, R. Jeanloz, Hysteresis in the high-pressure transformation of bcc- to hcp-iron, *J. Appl. Phys.* **69**, 6126 (1991)
- [4] S. Merkel, A. Goncharov, H. Mao, P. Gillet, R. Hemley, "Raman spectroscopy of iron to 152 gigapascals: Implications for Earth's inner core", *Science* **288**, 1626–1629 (2000).
- [5] A. F. Goncharov, V. V. Struzhkin, "Raman spectroscopy of metals, high-temperature superconductors and related materials under high pressure", *J. Raman Spectrosc.* **34**, 532–548 (2003).
- [6] B.W. Lebert, T. Gornia, M. Casula, S. Klotz, F. Baudalet, J.M. Ablett, T.C. Hansen, A. Juhin, A. Polian, P. Munsch, G. Le Marchand, Z. Zhang, J.P. Rueff, M. d'Astuto, "Epsilon iron as a spin smectic state", *Proceedings of the Nation Academy of Science* **116**, 20280–20285 (2019).
- [7] A. Monza, A. Meffre, F. Baudalet, J.-P. Rueff, M. d'Astuto, P. Munsch, S. Huotari, S. Lachaize, B. Chaudret, and A. Shukla, "Iron Under Pressure: "Kohn Tweezers" and Remnant Magnetism", *Phys. Rev. Lett.* **106**, 247201 (2011).
- [8] D. Jaccard, A.T. Holmes, "Spin and valence-fluctuation mediated superconductivity in pressurized Fe and  $\text{CeCu}_2(\text{Si/Ge})_2$ ", *Physica B* **359**, 333 (2005).
- [9] S. Gilder & J. Glenn, "Magnetic properties of hexagonal closed-packed Iron deduced from direct observations in a diamond anvil cell", *Science* **279**, 72 (1998).
- [10] G. Steinle-Neumann, L. Stixrude, R. E. Cohen, "Magnetism in dense hexagonal iron." *Proc. Natl. Acad. Sci. U.S.A.* **101**, 33–36 (2004).
- [11] S. Klotz, *Techniques in High Pressure Neutron Scattering*, Taylor & Francis / CRC Press, 2013.
- [12] S. Klotz, T. Strässle, B. Lebert, M. d'Astuto, T. Hansen, "High pressure neutron diffraction to beyond 20 GPa and below 1.8 K using Paris-Edinburgh load frames". *High Press. Res.* **36**, 73–78 (2016).
- [13] A. Zeidler, M. Guthrie, P.S. Salmon, "Pressure-dependent structure of the nullscattering alloy  $\text{Ti}_{0.676}\text{Zr}_{0.324}$ ", *High Press. Res.* **35**, 239–246 (2015)

- [14] E. Bourgeat-Lami, J.-F. Chapuis, J. Chastagnier, S. Demas, J.-P. Gonzales, M.-P. Keay, J.-L. Laborier, E. Lelièvre-Berna, O. Losserand, P. Martin, L. Mélési, A. Petoukhov, S. Pujol, J.-L. Ragazzoni, F. Thomas and X. Tonon, "Overview of the projects recently developed by the advanced neutron environment team at the ILL", *Physica B* **385–386**, 1303-1305 (2006).
- [15] J.A. Rodríguez-Velamázan, J. Campo, J. Rodríguez-Carvajal, P. Noguera, "XtremeD – A new neutron diffractometer for high pressure and magnetic fields at ILL developed by Spain", *Journal of Physics: Conf. Series* **352**, 012010-1-4 (2011).
- [16] H-K Mao, W.A. Basset, T. Takahashi, "Effect of Pressure on Crystal Structure and Lattice parameters of Iron up to 300 kbar", *J. Appl. Phys.* **38**, 272-276 (1967)
- [17] A. Dewaele, P. Loubeyre, F. Occelli, M. Mezouar, P. I. Dorogokupets, and M. Torrent, "Quasihydrostatic Equation of State of Iron above 2 Mbar", *Phys. Rev. Lett.* **97**, 215504 (2006).
- [18] P. Vinet, J. Ferrante, J. Rose, J. Smith, "Compressibility of solids", *J. Geophys. Res.* **92**, 9319–9325 (1987).
- [19] A. Dewaele, G. Garbarino, "Low temperature equation of state of iron", *Appl. Phys. Lett.* **111**, 2–6 (2017).
- [20] J. Rodriguez-Carvajal, "Recent advances in magnetic structure determination by neutron powder diffraction", *Physica B* **192**, 55–69 (1993).
- [21] G.L. Squires, *Introduction to the Theory of Thermal Neutron Scattering*, Cambridge University Press, Cambridge, 1978.
- [22] A. Cini, M. Mannini, F. Totti et al., "Mössbauer spectroscopy of a monolayer of single molecule magnets", *Phys. Nature Comm.* **9**, 480 (2018).
- [23] R. Khasanov, Z. Guguchia, A. Maisuradze *et al.*, "High pressure research using muons at the Paul Scherrer Institute", *High Press. Res.* **36**, 140–166 (2016).
- [24] C. Lacroix, Ph. Mendels, F. Mila (eds.), *Introduction to Frustrated Magnetism*, Springer Series in Solid-State Sciences (Springer-Verlag Berlin Heidelberg 2011), DOI 10.1007/978-3-642-10589-0
- [25] Ch. Pfleiderer, *Superconducting phases of  $f$ -electron compounds*, *Rev. Mod. Phys.* **81**, 1551 (2009) <https://doi.org/10.1103/RevModPhys.81.1551>